

DOI: 10.17617/2.3195201

Proceedings of the 9th Solar Polarization Workshop SPW9

A workshop held in Göttingen, Germany, from August 26 to August 30, 2019

Achim Gandorfer, Andreas Lagg, Kerstin Raab (eds.)

© The author(s) 2019. Published open access by MPS 2020

Polarization Calibration of the Solar Magnetic Activity Research Telescope (SMART) -T4

D. Yamasaki^{1,*}, S. Nagata², and K. Ichimoto²

¹Department of Astronomy, Kyoto University, Kitashirakawaoiwake, Sakyo-ku, Kyoto, 606-8502, Japan

²Hida Observatory, Kyoto University, Kurabashira, Takayama, Gifu, 506-1314, Japan

*Email: dyamasaki@kusastro.kyoto-u.ac.jp

Abstract. We report polarization calibration of the filter magnetograph of the Solar Magnetic Activity Research Telescope (SMART) at Hida Observatory. The polarimeter response matrix (Elmore 1990) derived from the experiment shows a significant spacial variation across the field of view especially on the crosstalk among the Stokes Q , U , and V . We discuss that the spacial variation might be caused by the linear and circular diattenuation of a polarizing beam splitter.

1 Introduction

1.1 Overview of the polarimeter

The Solar Magnetic Activity Research Telescope (SMART; UeNo et al. 2004) at Hida Observatory consists of four telescopes equipped on a unique equatorial mount. The fourth telescope T4 is a 250mm diameter partial disk filter magnetograph (Nagata et al. 2014).

One of the scientific goals of the T4 is to study the fluctuations of photospheric magnetic field during the solar flares with the time cadence of a minute or less and the polarimetric sensitivity of 5×10^{-4} . In order to achieve the time cadence and the sensitivity, we take more than 600 pairs of frames in 20 seconds to derive the Stokes vector in one wavelength.

The optical layout of the T4 is shown in figure 1. The polarization modulator of the T4 is a rotating waveplate placed just behind the primary focus. The waveplate is continuously rotating at the frequency of 1.7 Hz during the observations. We take the monochromatic images around the 6302.5 Å (Fe I) with a tandem Fabry-Perot filter (the bandwidth is ~ 130 mÅ). The polarization analyzer of the T4 is a polarizing beam splitter (PBS), with which we divide the beam into orthogonal polarized lights; we use the coordinate system that defines $+Q$ as the direction of p component of the PBS in this study. Two CCD cameras placed behind the PBS simultaneously take each of the orthogonally polarized lights with a frame rate of 30 frames per second.

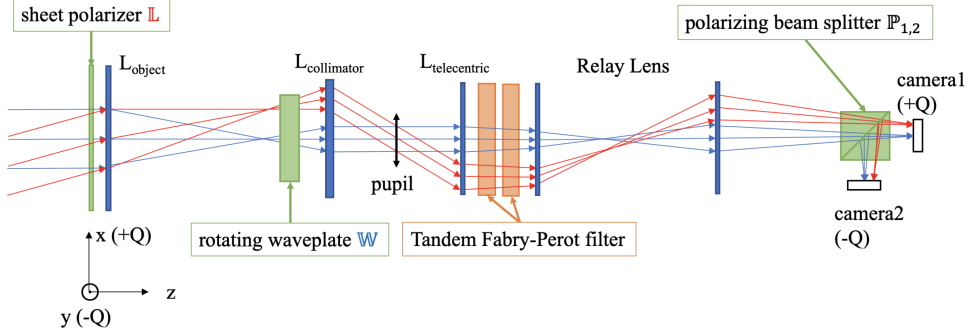


Figure 1. Optical layout of the T4. z-axis: incident light direction, x-axis: $+Q$, y-axis: $-Q$. The sheet polarizer just in front of the objective lens (L_{object}) is only used in polarization calibration.

1.2 Measurement of Stokes vector

The procedure to obtain the Stokes vectors with the T4 observation is explained in figure 2. We derive the Stokes vector \mathbf{S}_{out} based on the simple theoretical description of the instrumental polarization model as follows. The observed intensities of two cameras (I_{\pm}) can be given as the multiplication of the Mueller matrices of the polarization modulator and analyzer;

$$\begin{aligned}
 I_{\pm}(\theta) &= \begin{pmatrix} 1 \\ 0 \\ 0 \\ 0 \end{pmatrix} \cdot \mathbf{M}_{\mathbf{p}\pm} \cdot \mathbf{M}_{\mathbf{w}}(\theta) \cdot \begin{pmatrix} I_{in} \\ Q_{in} \\ U_{in} \\ V_{in} \end{pmatrix} \\
 &= \frac{1}{2} \{ I_{in} \pm \left(\frac{1 + \cos \delta}{2} + \frac{1 - \cos \delta}{2} \cos 4\theta \right) \times Q_{in} \\
 &\quad \pm \left(\frac{1 - \cos \delta}{2} \sin 4\theta \right) \times U_{in} \mp \sin \delta \sin 2\theta \times V_{in} \},
 \end{aligned} \tag{1}$$

where $\mathbf{M}_{\mathbf{p}\pm}$ are the Mueller matrices of the PBS, $\mathbf{M}_{\mathbf{w}}(\theta)$ is the Mueller matrix of the rotating waveplate at the rotating angle of θ , and δ is a retardation of the waveplate ($\delta \sim 127.0$ deg around 6302.5 \AA). Note that θ is given as a function of time $\theta(t) = \omega t$; ω is the angular frequency of the rotating waveplate.

The summation and subtraction of these intensities are follows;

$$\begin{aligned}
 I_+(\theta) + I_-(\theta) &= I_{in}, \\
 I_+(\theta) - I_-(\theta) &= \frac{1 - \cos \delta}{2} Q_{in} \times \cos 4\theta + \frac{1 - \cos \delta}{2} U_{in} \times \sin 4\theta - \sin \delta V_{in} \times \sin 2\theta.
 \end{aligned} \tag{2}$$

The advantage of the two orthogonal polarized beam measurement is that we can separate the time series of the I_{in} and $Q_{in}/U_{in}/V_{in}$. Thus we can suppress the crosstalk from the incident Stokes I to Stokes $Q/U/V$.

Based on the theoretical model given by equation (2) and (3), we derive the output Stokes vector \mathbf{S}_{out} by a sinusoidal fitting with θ , 2θ , and 4θ which correspond to the angular frequency of ω , 2ω and 4ω .

However, the actual Mueller matrix of the T4 deviates from the theoretical expression given above equation (1). Thus, we need to calibrate the \mathbf{S}_{out} to derive the Stokes vector of the Sun (\mathbf{S}_{in}).

$$\mathbf{S}_{\text{out}} = \mathbf{X}\mathbf{S}_{\text{in}}. \quad (4)$$

Here \mathbf{X} is the polarimeter response matrix (Elmore 1990). In other words, the purpose of polarization calibration is to examine the relationship between the known incident Stokes vector and the output corresponding to that input Stokes vector. Note that the polarimeter response matrix represents the crosstalk among the Stokes vector parameters $I/Q/U/V$, and those crosstalk is the systematic errors in polarimetry.

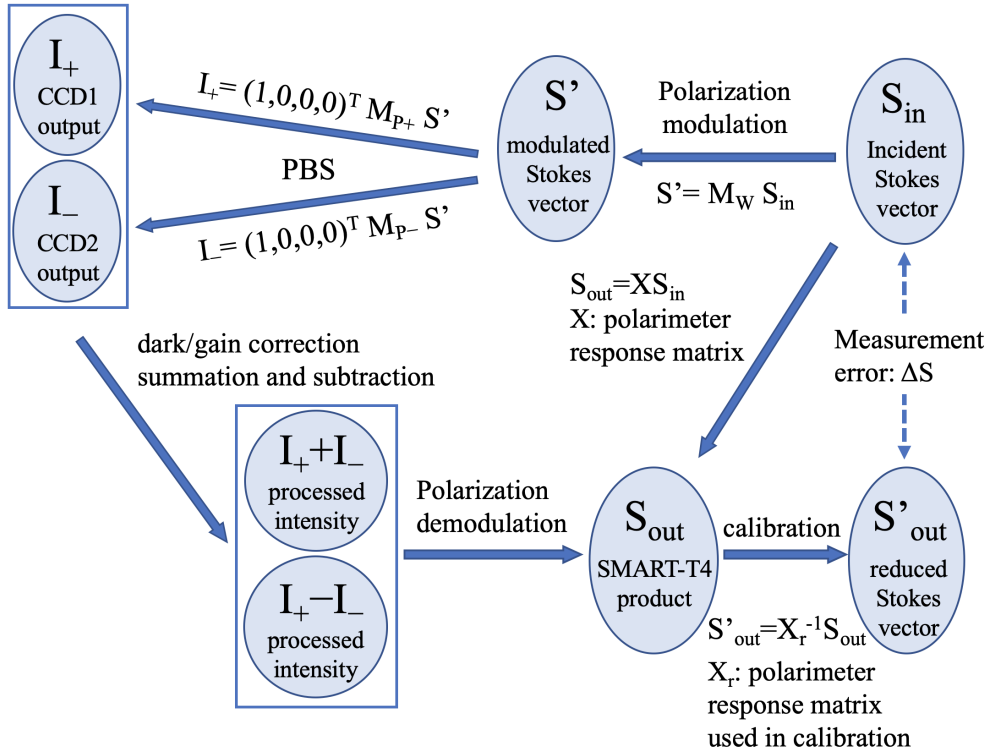


Figure 2. Definition of polarimeter response matrix and error in polarization measurement.

2 Experiment

2.1 On the accuracy and sensitivity of polarization measurement

Ichimoto et al. (2008) discusses the requirement on accuracy of the measurement of the polarimeter response matrix. The errors of the measured normalized Stokes parameter S/I ($= Q/I, U/I, \text{ and } V/I$) can be expressed by

$$\Delta\left(\frac{S}{I}\right) = \Delta_s\left(\frac{S}{I}\right) + \Delta_b, \quad (5)$$

where the first term is the systematic error – “scale error”, and the second term is the statistical error – “bias error”. Here we note that the error in polarization calibration is the error of the measured polarimeter response matrix \mathbf{X} . Thus the “scale error” in equation (5) can be described as

$$\Delta\left(\frac{S}{I}\right) = (\mathbf{X}_r^{-1}\mathbf{X} - \mathbf{E})\left(\frac{S}{I}\right), \quad (6)$$

where \mathbf{X} is the true polarimeter response matrix, \mathbf{X}_r is the measured one, and \mathbf{E} is the identity matrix.

We require that the Δ_s and Δ_b to be smaller than the scale error a and the photometric noise ε , respectively. Thus, the requirement is given as the following equation,

$$\|\mathbf{X}_r^{-1}\mathbf{X} - \mathbf{E}\| = \|\Delta\mathbf{X}\| < \begin{pmatrix} - & a/P_l & a/P_l & a/P_c \\ \varepsilon & a & \varepsilon/P_l & \varepsilon/P_c \\ \varepsilon & \varepsilon/P_l & a & \varepsilon/P_c \\ \varepsilon & \varepsilon/P_l & \varepsilon/P_l & a \end{pmatrix}, \quad (7)$$

where P_l and P_c are the expected maximum linear- and circular-polarization degrees in the solar spectra, respectively (See also Anan et al. 2018).

For T4’s polarization calibration, we adopt $\varepsilon = 0.001$, $a = 0.05$, $P_l = 0.15$, and $P_c = 0.20$ for the accuracy requirement, and the tolerance matrix is shown in below;

$$\|\Delta\mathbf{X}\| < \begin{pmatrix} - & 0.333 & 0.333 & 0.250 \\ 0.001 & 0.050 & 0.007 & 0.005 \\ 0.001 & 0.007 & 0.050 & 0.005 \\ 0.001 & 0.007 & 0.007 & 0.050 \end{pmatrix}, \quad (8)$$

this requirement is as high as that of Hinode/SOT.

2.2 Experiment setup and data analysis

We carried out polarization calibration of the T4 with linear- and circular-sheet polarizers placed in front of the telescope (figure 1). We investigated the polarimeter response matrix at the four wavelengths of $6302.5 \text{ \AA} \pm 0.080 \text{ \AA}$, $\pm 0.160 \text{ \AA}$. The detail of the experiment is shown in table 1.

In the data analysis, we at first fitted the observed intensities I_{\pm} with the sinusoidal fitting function and corrected the gain of two cameras. Figure 3 shows an example of the fitting for the incident Stokes vector $\mathbf{S}_{in} = (1, 1, 0, 0)^T$. In the figure, we can clearly find significant signals in $\cos 4\theta$ amplitude, which corresponds to the input in this measurement, Q_{in} . We also find the difference between two cameras; the difference of the gain of the cameras. We performed the same analysis for $\pm Q$, $\pm U$, and $\pm V$ measurements. By using the spacial distribution of the significant outputs corresponding to these six input Stokes vectors, we corrected the gain of two cameras.

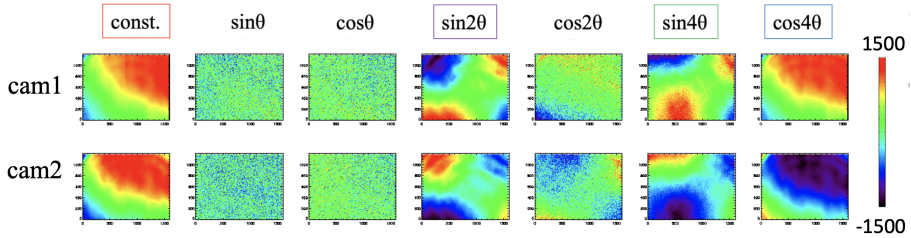


Figure 3. Coefficient maps through the T4's field of view in case of -0.16 \AA from wavelength center with $+Q$ input, upper and bottom panels correspond to camera1 and camera2 respectively.

We then derived the output Stokes vectors ($\mathbf{S}_{out,m} = (I_{out,m}, Q_{out,m}, U_{out,m}, V_{out,m})^T$) for each input $m (= 1, \dots, 32)$ with the theoretical model given in section 1.2. The known input Stokes vectors ($\mathbf{S}_{in,m} = (I_{in,m}, Q_{in,m}, U_{in,m}, V_{in,m})^T$) for each measurement $m (= 1, \dots, 32)$ were simply calculated as follows;

$$\mathbf{S}_{in,m} = \mathbf{M}_{pol,m} \cdot I_{out,m} \cdot \begin{pmatrix} 1 \\ 0 \\ 0 \\ 0 \end{pmatrix}, \quad (9)$$

where $\mathbf{M}_{pol,m}$ correspond to the Mueller matrices of the polarizer that set in front of the telescope for each input $m (= 1, \dots, 32)$. Here we note that we assumed the incident Stokes vector to the polarizers in front of the telescope as the natural unpolarized light, $(1, 0, 0, 0)^T$.

We at last derived the polarimeter response matrix (\mathbf{X}_r) from the equation below:

$$\mathbf{S}_{in,m} = \mathbf{X}_r^{-1} \cdot \mathbf{S}_{out,m}. \quad (10)$$

Table 1. Overview of the experiment

| polarizer | date | # of input Stokes vector | exp. time | target |
|-----------|------------|--------------------------|----------------|-------------|
| HN38 | 2019-05-23 | 16 ¹ | 4000 μ sec | disk center |
| HNCP37R | 2019-05-24 | 8 ² | 4000 μ sec | disk center |
| HNCP37L | 2019-05-24 | 8 ³ | 4000 μ sec | disk center |

2.3 Results and discussion

Figure 4 displays the reduced polarimeter response matrix as a function of the T4's field of view. Each panel corresponds to each component of the polarimeter response matrix. We find the significant spacial variation across the field of view. In order to discuss the spatial

¹The polarizer angle was set at $0.00, \pm 11.25, \pm 22.50, \pm 33.75, \pm 45.00, \pm 56.25, \pm 67.50$, and 90.00 deg from the original position of the polarizer.

²The polarizer angle was set at $0.00, \pm 22.50, \pm 45.00, \pm 67.50$, and 90.00 deg from the original position of the polarizer.

³The polarizer angle was set at $0.00, \pm 22.50, \pm 45.00, \pm 67.50$, and 90.00 deg from the original position of the polarizer.

distribution quantitatively, we calculate the standard deviation of the each component across the field of view ($\sigma \mathbf{X}_r^{-1}$),

$$\sigma \mathbf{X}_r^{-1} = \begin{pmatrix} - & 0.000 & 0.000 & 0.000 \\ 0.002 & 0.084 & 0.030 & 0.014 \\ 0.001 & 0.031 & 0.084 & 0.010 \\ 0.003 & 0.070 & 0.013 & 0.078 \end{pmatrix}.$$

Some of these values are larger than the requirements given in equation (8). In other words, we can not regard the obtained polarimeter response matrix as uniform across the field of view. Thus, we need to calibrate the output Stokes vectors pixel to pixel.

On the other hand, as shown in figure 4, the T4's polarimeter response matrix of crosstalk between Q and U (X_{23}^{-1} and X_{32}^{-1}) and crosstalk from Q/U to V (X_{42}^{-1} and X_{43}^{-1}) show the similar spacial distribution.

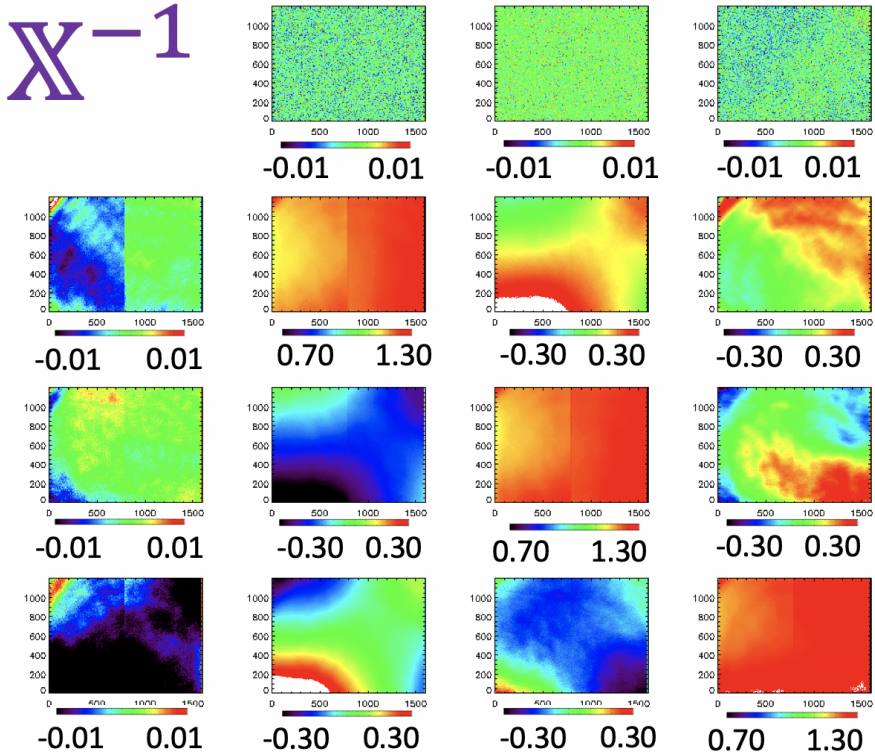


Figure 4. Polarimeter response matrix \mathbf{X}_r^{-1} map through the T4's field of view.

The spacial distributions in these components can be explained if we assume that the PBS has linear and circular diattenuation. By taking into account those diattenuation of the PSB, the intensities (I''_{\pm}) are modified as follows,

$$I''_{\pm}(\theta) = \frac{1}{2} \{ I_{in} \pm \left(\frac{1 + \cos \delta}{2} + \frac{1 - \cos \delta}{2} \cos 4\theta \right) \}$$

$$\begin{aligned}
& + P_{13} \frac{1 - \cos \delta}{2} \sin 4\theta + P_{14} \sin \delta \sin 2\theta) \times Q_{in} \\
& \pm \left(\frac{1 - \cos \delta}{2} \sin 4\theta + P_{13} \frac{1 + \cos \delta}{2} \right. \\
& - P_{13} \frac{1 - \cos \delta}{2} \cos 4\theta - P_{14} \sin \delta \cos 2\theta) \times U_{in} \\
& \mp (\sin \delta \sin 2\theta + P_{13} \sin \delta \cos 2\theta + P_{14} \cos \delta) \times V_{in}, \tag{11}
\end{aligned}$$

where P_{13} and P_{14} are linear and circular diattenuation respectively.

The results are shown in figure 5. We find the significant spatial patterns of the linear and circular diattenuation as expected.

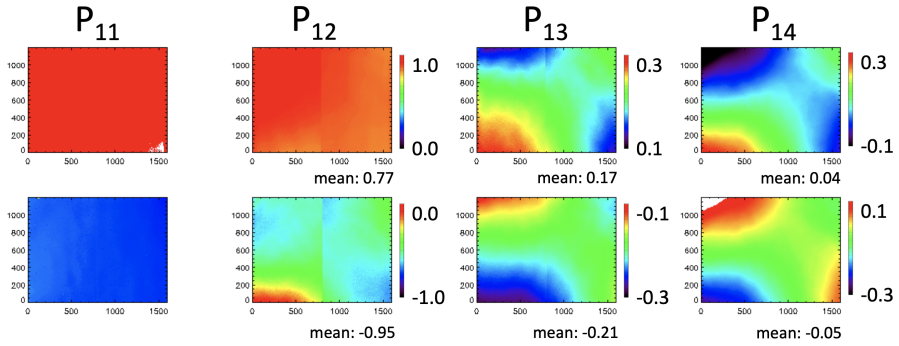


Figure 5. Estimated first column of the PBS Mueller matrices, upper and lower panels correspond to the transmission and reflection direction of the PBS respectively. P_{ij} corresponds to the ij component of the PBS’s Mueller matrices.

3 Summary

We performed end-to-end polarization calibration on the SMART-T4 with linear and circular polarizers to examine the polarimeter response matrix. Some components of the polarimeter response matrix contain significant spatial distributions, which are larger than the requirements. Thus, we need to calibrate the T4 Stokes vector products pixel to pixel. The spatial patterns of the T4’s polarimeter response matrix can be explained by the $\sim 10\%$ of linear diattenuation and $\sim 1\%$ circular diattenuation of the PBS.

Acknowledgement. This work was supported by the “UCHUGAKU” project of the Unit of Synergetic Studies for Space, Kyoto University and by JSPS KAKENHI 20684005, Grant-in-Aid for Young Scientist (A).

References

- Anan, T., Huang, Y.-W., Nakatani, Y., et al. 2018, Publications of the Astronomical Society of Japan, 70, 102
 Elmore, D. F. 1990, NCAR Technical Note NCAR/TN-355+STR
 Ichimoto, K., Lites, B., Elmore, D., et al. 2008, Solar Physics, 249, 233

- Nagata, S., Morita, S., Ichimoto, K., et al. 2014, Publications of the Astronomical Society of Japan, 66, 45
- UeNo, S., ichi Nagata, S., Kitai, R., Kurokawa, H., & Ichimoto, K. 2004, in Ground-based Instrumentation for Astronomy, ed. A. F. M. Moorwood & M. Iye, Vol. 5492, International Society for Optics and Photonics (SPIE), 958 – 969